Nanotechnology **19** (2008) 424007 (7pp) doi:10.1088/0957-4484/19/42/424007

Factors determining the photovoltaic performance of a CdSe quantum dot sensitized solar cell: the role of the linker molecule and of the counter electrode

Iván Mora-Seró[1,3], Sixto Giménez[1], Thomas Moehl[1], Francisco Fabregat-Santiago[1], Teresa Lana-Villareal[2], Roberto Gómez[2] and Juan Bisquert[1,3]

[1] Departament de Física, Universitat Jaume I, 12071 Castelló, Spain
[2] Departament de Química-Física i Institut Universitari d'Electroquímica, Universitat d'Alacant, Apartat 99, E-03080 Alacant, Spain

E-mail: sero@fca.uji.es and bisquert@fca.uji.es

Received 4 April 2008, in final form 25 April 2008
Published 25 September 2008
Online at stacks.iop.org/Nano/19/424007

Abstract
Colloidal CdSe quantum dots (QDs) of different sizes, prepared by a solvothermal route, have been employed as sensitizers of nanostructured TiO_2 electrode based solar cells. Three different bifunctional linker molecules have been used to attach colloidal QDs to the TiO_2 surface: mercaptopropionic acid (MPA), thioglycolic acid (TGA), and cysteine. The linker molecule plays a determinant role in the solar cell performance, as illustrated by the fact that the incident photon to charge carrier generation efficiency (IPCE) could be improved by a factor of 5–6 by using cysteine with respect to MPA. The photovoltaic properties of QD sensitized electrodes have been characterized for both three-electrode and closed two-electrode solar cell configurations. For three-electrode measurement a maximum power conversion efficiency near 1% can be deduced, but this efficiency is halved in the closed cell configuration mainly due to the decrease of the fill factor (FF).

(Some figures in this article are in colour only in the electronic version)

1. Introduction

Since the demonstration of the dye sensitized solar cell (DSC) concept [1], molecular sensitized nanostructured metal oxides have attracted significant attention as photoanodes in low-cost photovoltaic devices [2, 3]. The photosensitizer plays an important role in determining the stability, light harvesting capability and also the total cost of DSCs. At present, the most important photosensitizers are ruthenium dyes, but an intense research effort is focused on obtaining cheaper alternative panchromatic sensitizers. Semiconductor quantum dots (QDs) could provide one of the solutions due to their tunable band gap, by the increase of quantum confinement at decreasing quantum dot size [4]. Additionally, QDs exhibit a larger extinction coefficient than conventional dyes [4, 5], making them highly interesting as photosensitizers.

The use of QDs as photosensitizers has been spurred on in the past years due to the demonstration of extremely efficient carrier multiplication in colloidal QDs of PbS, PbSe and CdSe with internal quantum efficiency higher than 100% [6–9]. Such a multiplication is due to impact ionization [10], reaching even seven excitons per absorbed high-energy photon in PbSe colloidal nanocrystals [6, 9]. One of the possible solar cell configurations to take advantage of this phenomenon is the quantum dot sensitized solar cell (QDSC) [6, 11]. However, it has not been shown so far that multiple carriers could be injected in external media. Therefore, an improved understanding of QDSCs is needed in order to design the appropriate cell configuration in which this effect could be used.

[3] Authors to whom any correspondence should be addressed.

Part of the work realized in the last two decades on conventional DSCs can be applied to the development of QDSCs, although some new parameters or reformulated ones with respect to conventional DSCs have to be taken into account to optimize QDSCs. There are several works studying different types of QD as photosensitizers; for example, InP [12], PbS [13, 14], Bi_2S_3 [13, 15], InAs [16], CdS [13, 17] or CdSe [18–23]. In particular, CdSe QDs have received special attention due to their relatively easy synthesis and also because the tuneable band edge offers the opportunity to harvest light energy in most of the visible region of the solar spectrum. In this sense, they are appropriate sensitizers to check the QDSC concepts. This work will focus on two important aspects of CdSe QDSCs, namely, the role of the molecular linkers to improve photocarrier harvesting from QDs, and the comparison of the characteristics of photoanodes and complete solar cells.

In order to sensitize large band gap semiconductors such as TiO_2 or ZnO with CdSe QDs, two main methods have been employed:

(i) growing of the QDs directly on the large band gap semiconductor surface [18, 23], or
(ii) linking previously synthesized colloidal QDs with a bifunctional molecule [19–22].

The highest cell efficiencies have been attained with the former method. Niitsoo *et al* [18] reported an efficiency of 2.8% under 1 sun illumination in a three-electrode configuration, for chemical bath deposited CdS/CdSe sensitized porous TiO_2 solar cells. Diguada *et al* [23] obtained a cell efficiency of 2.7% but now in a closed cell configuration (two-electrode system), even though in this case the FFs obtained are poor, lower than 0.45 for the majority of the samples. In both works, a polysulfide electrolyte has been used as the redox couple to regenerate the photoexcited holes in the QDs. Polysulfide electrolyte is used instead of the I_3^-/I^- redox couple usually employed in the conventional DSCs in order to maintain the stability of CdSe [24, 25]. It should be remarked that in the three-electrode configuration, the role of the counter electrode is not taken into account, and in a two-electrode system, such as a practical solar cell, the performance would be considerably decreased. In this work we will show that the charge transfer between the polysulfide redox couple and the platinized transparent conducting counter electrode possesses a high charge transfer resistance, affecting the cell performance via reduction of the fill factor (FF).

The second method allows a careful control of the QD properties, like size and shape, by the colloidal synthesis, which is not possible with the direct growth of QDs on the semiconductor surface. Additionally, it is an efficient way to save precursor material because only the attached QDs are used and the remaining QDs in the solution can be stored for another use. Kamat and co-workers proposed this method [19] and checked the effect of three different molecules, namely, mercaptopropionic acid (MPA), thiolacetic acid (TAA) and mercaptohexadecanoic acid (MDA), obtaining the best results for MPA. All these molecules possess a thiol group, SH, that links to the QDs via a Cd–S bond, and another carboxylate group, COOH, that links to the TiO_2. Other authors have employed MPA to link CdSe QDs to ZnO nanowires [21], or thioglycolic acid (TGA) [20] to link CdSe to TiO_2. Kamat and co-workers showed [19] that the linker molecule used can affect the solar cell performance.

Cysteine has not been used previously, as far as we know, as a linker molecule to attach QDs to large band gap semiconductors. This amino acid plays a significant role in natural and artificial systems related to energy conversion catalysis. Via its three functional groups (thiol, amino, and carboxyl), it is capable of interacting easily with molecules and surfaces, and since this molecule is small, these functional groups induce high charge density on a small area. Cysteine functions in nature in several redox proteins as a linker between the metal based inorganic reaction centre and the protein matrix. As an example, in ferredoxin it acts as an electron transfer bridge between the Fe_4S_4 cubane cluster and the protein backbone [26, 27]. Moreover, it was found that these kinds of cysteine bridge in nature are resistant to evolutionary mutation, indicating that this amino acid has, in comparison to the other possible linking amino acids, superior capabilities regarding charge transfer [26]. In artificial self-assembled monolayer (SAM) based biosensors, cysteine is also used as a coupling chain between the inorganic and biological components. It adsorbs with its thiol group on gold and forms an SAM. The other functional groups are used to immobilize redox proteins such as copper–zinc superoxide dismutase (SOD), enabling redox reactions with the metal electrode and the protein, which would not even take place without the linking molecule [28]. Likewise, this molecule is capable of promoting redox reactions, for example of hydroquinone with gold [29].

There are several reports on the interaction of cysteine with semiconductors. Adsorbed on titanium dioxide, cysteine enhances the light induced reduction of heavy metals along with the destructive oxidation of organic compounds [30, 31], which involves, in both cases, charge transfer via the amino acid. Adsorbed on n-MoS_2, this amino acid can reduce unfavourable photocorrosion reactions, whereby it enhances charge transfer between the semiconductor and the redox couple, leading to an increase of favourable photocurrent [32, 33]. These results from the literature demonstrate the favourable properties of this molecule as a linker for two building blocks of charge-mediating devices, enforcing it as a candidate for the investigation of the interaction of QDs linked to wide band gap semiconductor oxides.

In the present study we compare the effect of three different linkers, MPA, TGA and cysteine, obtaining that the incident photon to charge carrier generation efficiency (IPCE) can be improved by a factor of 5–6 if cysteine is used as a linker instead of MPA in CdSe QDSCs.

2. Experimental details

2.1. Preparation of CdSe QDs

CdSe QDs, capped with trioctylphosphine (TOP), were prepared by a solvothermal route that allows size control [34].

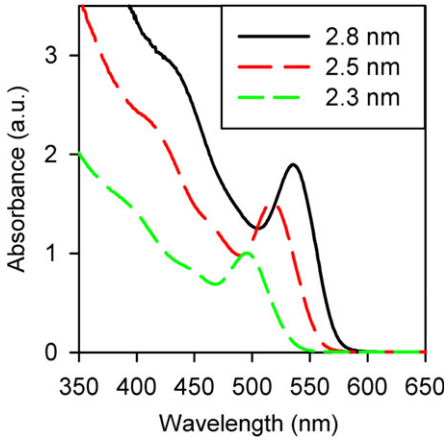

Figure 1. UV–vis absorption spectrum of colloidal CdSe QDs in toluene solution after purification, prepared with three different reaction times, 15, 5 and 2.5 h, corresponding to three different quantum dot sizes, 2.8, 2.5 and 2.3 nm, respectively.

Briefly, selenium reacts with cadmium myristate in toluene in the presence of oleic acid and TOP. The reaction takes place at 180 °C in a sealed autoclave. By changing the reaction time, different sizes of quantum dots were obtained. The as-prepared colloidal solutions were characterized by a Shimadzu UV-2401 PC. In the case of photoelectrochemical measurements, the CdSe quantum dots were previously purified by precipitation in ethanol, isolation by centrifugation and decantation, three times. Figure 1 shows the absorption spectra of the three QD dispersions with different QD sizes employed in this study. The QDs were synthesized over 2.5, 5 and 15 h. The changes in the wavelength of the absorption peak reflects the size quantization confinement, the peak shifting to lower wavelengths as the QD size decreases. Comparing the absorption peak maximum (495, 517 and 536 nm) corresponding to the first excitonic transition with the curves reported by Peng and co-workers [4], the QD diameters could be obtained (2.3, 2.5 and 2.8 nm, respectively).

2.2. Preparation of QD sensitized electrodes

Colloidal TiO_2 paste (20–400 nm particle size) was supplied by ECN (Petten, The Netherlands). 1×1 cm^2 TiO_2 films were deposited on SnO_2:F (FTO) coated glass electrodes (Pilkington TEC15, 15 Ω/sq resistance) by the doctor blade technique and subsequently sintered at 450 °C for 30 min in a muffle-type furnace. The sintered TiO_2 film thickness was of 10 μm, as measured by a profilomer Dektack 6 (Veeco).

Three different solutions were prepared to attach the linker molecules to the TiO_2 surface. For MPA and TGA a solution (1:10) in acetonitrile was prepared, while for cysteine a saturated solution in toluene was employed. All the linkers were provided by Aldrich; their molecular structures are shown in figure 2. After sintering, the FTO/TiO_2 electrodes were immersed in the solution containing the linker molecules for at least 24 h, rinsed with the same solvent and dipped in the CdSe/TOP/toluene solution for at least 24 h.

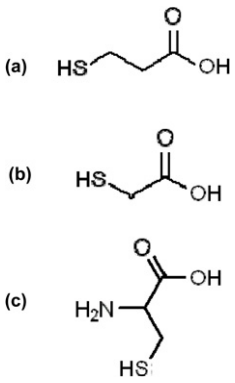

Figure 2. The molecular structure of (a) MPA; (b) TGA and (c) cysteine.

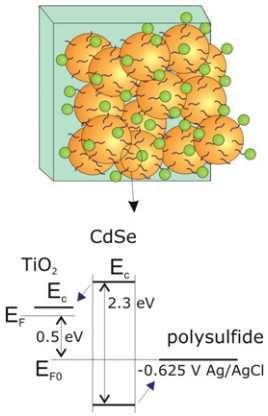

Figure 3. Scheme of TiO_2 nanoparticle film sensitized with quantum dots attached by organic linker molecules. The diagram shows the main energy levels involved in the charge transfer of electrons and holes from the quantum dot to the semiconductor matrix and redox couple, respectively. E_c denotes the conduction band level and E_F denotes the Fermi level. The band gap of 2.3 eV corresponds to the largest quantum dots used, of 2.8 nm diameter.

2.3. Solar cell configuration

The QD sensitized electrodes were characterized in two different solar cell configurations with three and two electrodes. For the three-electrode configuration a standard three-electrode cell using a Ag/AgCl (in aqueous KCl 3 M) reference electrode and a Pt wire counter electrode was used. The closed cell configuration (two-electrode system) was prepared by assembling a thermally platinized FTO counter electrode and a QD sensitized FTO/TiO_2 electrode using a thermoplastic frame (Dupont™ Surlyn®1702, thickness 25 μm). The Na_2S_x redox electrolyte was prepared following the procedure described in [35]: it was a 1 M Na_2S, 0.1 M S, and 0.1 M NaOH solution in Milli-Q ultrapure water. The electrolyte was introduced into the closed two-electrode cell through a hole drilled in the counter electrode, which was sealed after filling. Figure 3 shows the photoanode structure and the energy levels of the prepared solar cells.

2.4. Optical and electrical characterization

Current–potential curves and electrochemical impedance spectroscopy (EIS) data were obtained using an FRA equipped

PGSTAT-30 from Autolab. Current–potential curves were obtained using a halogen lamp for the three-electrode configuration. For the closed cell configuration the cells were illuminated using a solar simulator equipped with a 1000 W ozone-free xenon lamp and AM 1.5 G filter (Oriel), where the light intensity was adjusted with an NREL calibrated Si solar cell with a KG-5 filter to 1 sunlight intensity (100 mW cm^{-2}). EIS measurements were done in the three-electrode cell configuration applying a 20 mV AC sinusoidal signal over the constant applied bias with the frequency ranging between 500 kHz and 5 mHz. IPCE measurements were performed employing a 150 W Xe lamp coupled with a monochromator controlled by a computer; the photocurrent was measured using an optical power meter 70310 from Oriel instruments. The IPCE measurements were corrected considering the reflection in the glass/FTO substrate.

3. Results and discussion

IPCE measurements of QDSCs with QDs of 2.8 nm diameter were carried out in the closed cell configuration using MPA, TGA and cysteine as bifunctional molecules to attach the QDs to TiO_2 surface; see figure 4(a). The IPCE patterns are similar for the three linkers and in good correlation with the absorbance measurements; see figure 1. A significant difference is observed in the IPCE values if TGA or cysteine are used instead of MPA, obtaining the best results with cysteine. The IPCE value at the peak maximum, placed at the same positions as the absorbance peaks, are 4.2, 10.5 and 23.2 for MPA, TGA and cysteine, respectively. It is known that the selection of the linker to fix the colloidal QD plays a determinant role in the cell performance [19]. Vanmaekelbergh and co-workers [36] have characterized colloidal CdSe QDs chemisorbed on a gold electrode using a variety of SAMs consisting of dithiols and rigid disulfides, observing that the tunnelling rate between the CdSe QDs and Au substrate depends exponentially on the distance. In our case, the three investigated linkers are closely related structurally. As expected, the efficiency for TGA is higher (about double) compared to that for MPA. The tunnelling probability is reduced [36] due to the longer molecular base chain by one sp^3 hybridized C element in MPA, leading to the observed decrease of electron injection. Thus, by plain consideration of the length of the linking molecule, TGA should provide the highest observed efficiencies. Instead, the IPCE for the CdSe QDs linked with cysteine to the semiconductor surface reveals the highest photon conversion efficiency (about five to six times more in comparison to MPA and about double compared to TGA).

While cysteine has been widely investigated [26] in proteins, it has not been agreed yet why it is such a good charge transfer mediating molecule. The amino group, and, in particular, its electron donating capabilities and/or its possibility of protonation, seem to play a significant role in this process, since it is the only difference between MPA and cysteine. Electron paramagnetic resonance (EPR) investigations also show that cysteine adsorbed on TiO_2 can trap an electron or a hole, forming a cysteine radical,

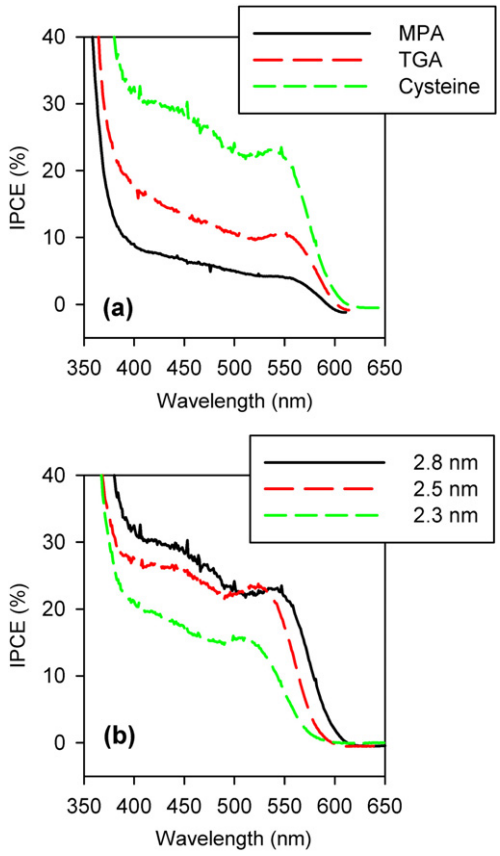

Figure 4. Incident photon to charge carrier generation efficiency (IPCE) measured in the closed cell configuration (two-electrode system): (a) comparison using the same QDs as sensitizers (2.8 nm) and three different linker molecules: MPA, TGA and cysteine; (b) comparison using three different quantum dot sizes using cysteine as a linker.

demonstrating the good stabilization of charges in this molecule [30]. Thus, the reasons for the good charge transfer properties of this amino acid might rely on the high electron density over the molecular structure and the good donor–acceptor abilities of the free electron pair of the amino group. Moreover, an adsorption configuration that is different from that of MPA, caused by the presence of the amino group, cannot be discarded. In particular, cysteine could anchor to the QD via both the thiol and the amino groups. In such a way, the distance between the oxide particle and the QD would slightly decrease. As another explanation, one should be aware that cysteine as an amino acid can be present as a zwitterionic structure, giving rise to a linker molecule with a strong dipole close to the QD. This may create locally a strong stabilization of the charge separated states, and thus the behaviour observed.

Following these results cysteine has been used as a linker molecule in the further experiments that we discuss, unless otherwise stated. The IPCEs for the closed cell configuration using QDs with different sizes are plotted in figure 4(b). There is a close correlation between IPCE and absorbance measurements, figure 1, indicating a correlation between absorption in the CdSe QDs and injection into TiO_2, as has been shown by other techniques, such as surface photovoltage spectra [37].

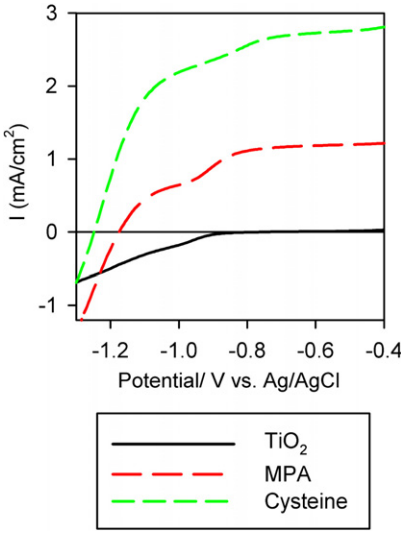

Figure 5. Current–potential curves for two electrodes sensitized with CdSe QDs (2.8 nm) using MPA and cysteine as linker molecules and for a bare TiO_2 nanostructured electrode measured in a three-electrode configuration under 1 sun illumination.

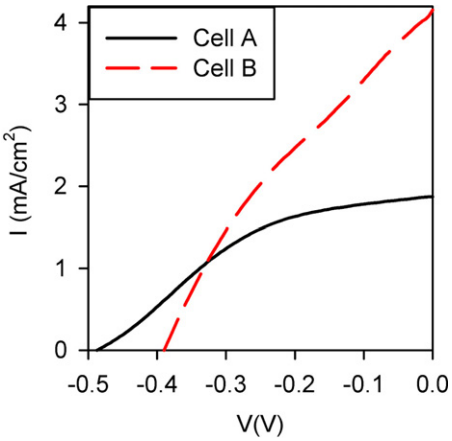

Figure 6. Current–potential curves for cells A and B sensitized with CdSe QDs (2.8 nm) using cysteine as the linker molecule measured in the closed cell configuration (two-electrode system).

Table 1. Photovoltaic properties of two different cells in the closed cell configuration (two-electrode system) under 1 sun illumination (AM 1.5 G).

Cell	V_{oc} (V)	I_{sc} (mA cm^{-2})	FF	η (%)
A	−0.490	1.87	0.43	0.40
B	−0.390	4.16	0.33	0.55

Current–potential curves using the three-electrode configuration have been measured under 1 sun illumination for a bare TiO_2 nanostructured electrode and for two electrodes sensitized with CdSe QDs (2.8 nm) using MPA and cysteine as linker molecules; see figure 5. The effect of QD sensitization is clearly observed in the photocurrent obtained under illumination. As expected from the IPCE results, figure 4(a), higher cell performance is obtained when cysteine is used as the linker. Taking into account the open circuit voltage in dark conditions with respect to the reference electrode, $V_{OC}^{Dark} = -0.625$ V versus Ag/AgCl, the electrode linked with cysteine exhibits a V_{OC} of 0.620 V under 1 sun illumination, with a short circuit current $I_{SC}^{V=-0.625\ V} = 2.67$ mA cm^{-2}, FF = 0.54 and a power conversion pseudo-efficiency of 0.92%. We use the prefix 'pseudo' to differentiate the efficiency calculated in three-electrode configuration, that does not take into account the effect of the counter electrode, from the power conversion efficiency, η, obtained in a practical, closed cell configuration with two electrodes. The pseudo-efficiency calculated for the electrode using MPA as a linker is 0.20%, 4.5 times lower than that obtained for the cysteine linked electrode, in good correspondence with the reduction in the IPCE observed in figure 4(a).

The closed cell configuration has also been investigated for CdSe QD (2.8 nm) sensitizers. In table 1, two examples of the photovoltaic properties obtained for closed cells under 1 sun illumination (AM 1.5 G) are shown. The current–potential curves obtained for cells A and B are also plotted in figure 6. The main difference between cell A and cell B is the TiO_2 paste: cell A was prepared using the procedure indicated in section 2, while cell B was prepared using a TiO_2 paste DSL18NR-AO from Dyesol. Additionally, the FTO contacts of the electrode and counter electrode of cell A were made using a tin alloy applied with an ultrasonic soldering system USS-9200 from MBR Electronics. It reduces the series resistance and allows us to obtain higher FFs.

Closed cells present an efficiency that is halved with respect to the three-electrode configuration, indicating a limiting effect of the counter electrode in the cell performance. The obtained FFs are very low in the closed cell configuration, see table 1, compared with those for the three-electrode configuration. Indeed, this parameter undergoes the highest reduction. This also indicates a limitation of the counter electrode. In order to analyse the role of the counter electrode, we have measured the electrochemical impedance spectra of a Pt wire as the working electrode in a three-electrode configuration with a standard three-electrode cell using Ag/AgCl (in aqueous KCl 3 M) as the reference electrode and a Pt wire as the counter electrode. The working electrolyte was the polysulfide electrolyte employed with the QDSCs. The measurement was carried out in dark conditions at different DC potentials versus Ag/AgCl. A semiarc corresponding to charge transfer between the Pt working electrode and the polysulfide redox couple has been identified in EIS measurements and characterized, obtaining the charge transfer resistance plotted in figure 7. The charge transfer resistance presents a maximum at $V = -0.750$ V versus Ag/AgCl, which is the closest value to $V_{OC}^{Dark} = -0.730$ V versus Ag/AgCl measured by impedance. As may be seen in figure 7, R_{ct-Pt} is governed by the classical Butler–Volmer relation:

$$j = j_0\left[\exp\left(\frac{\alpha e}{kT}(V - V_{ref})\right) - \exp\left(-\frac{(1-\alpha)e}{kT}(V - V_{ref})\right)\right] \quad (1)$$

where j is the charge transfer current density, j_0 is the exchange current density, V the applied potential, V_{ref} the

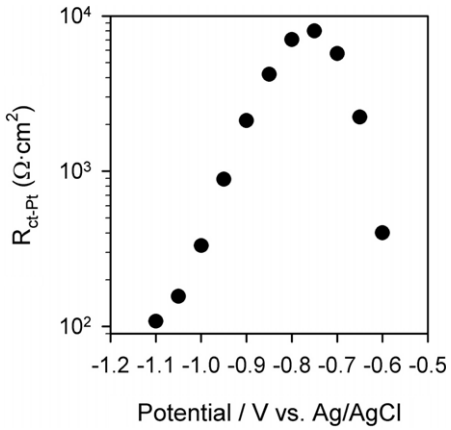

Figure 7. Charge transfer resistance between a platinum wire and polysulfide electrolyte measured in the three-electrode configuration.

reference potential (ideally the equilibrium potential for the redox couple), e the elementary charge, T the temperature, k the Boltzmann constant and α the asymmetry parameter. The value measured by impedance is related to the current density through the derivate [38],

$$R_{\mathrm{ct-Pt}} = \left(\frac{\mathrm{d}j}{\mathrm{d}V}\right)^{-1} \tag{2}$$

where $R_{\mathrm{ct-Pt}}$ has units of Ω cm^2. For negative potentials from V_{ref}, in our case $V_{\mathrm{OC}}^{\mathrm{Dark}}$, this becomes

$$R_{\mathrm{ct-Pt}} = \frac{(1-\alpha)e}{kTj_0} \exp\left(\frac{(1-\alpha)e}{kT}(V - V_{\mathrm{OC}}^{\mathrm{Dark}})\right), \tag{3}$$

and for potentials more positive than $V_{\mathrm{OC}}^{\mathrm{Dark}}$,

$$R_{\mathrm{ct-Pt}} = \frac{\alpha e}{kTj_0} \exp\left(-\frac{\alpha e}{kT}(V - V_{\mathrm{OC}}^{\mathrm{Dark}})\right). \tag{4}$$

The sum of the obtained negative and positive slopes in a natural log plot should theoretically give 40 V^{-1} at room temperature. In our case, a value of 44 V^{-1} (10% error) is obtained, with $\alpha = 0.38$. The calculated values for exchange currents, $j_0 = 11.4$ nA cm^{-2} obtained for polysulfide, is three orders of magnitude lower that the value of 40.7 μA cm^{-2} obtained for the I_3^-/I^- redox couple. Therefore, the obtained exchange current values for the Pt/polysulfide system are rather small, and this introduces a series resistance that negatively affects the solar cell performance. This effect is not observed in conventional DSCs, where the charge transfer resistance between the platinized FTO counter electrode and the I_3^-/I^- redox couple is significantly lower. It is likely that S in the polysulfide solution attaches to Pt in the counter electrode, poisoning it, and, consequently, increasing the charge transfer resistance. Our results are in agreement with those found in the literature [39, 40], pointing to the poor electrocatalytic activity of platinum. More importantly, these works highlight the good electrocatalytic activity of a particular cathode material, namely CoS, for the polysulfide couple. Further research using these alternative counter electrodes is planned in order to optimize QDSCs.

4. Conclusions

QDs have the potential to be used as TiO_2 sensitizers, but some new parameters such as the linker type or certain solar cell elements, which are well established in conventional DSC as the counter electrode, need to be optimized in order to increase the photovoltaic performance. In this respect, we have observed that the use of cysteine as a bifunctional molecular linker between colloidal CdSe QDs and TiO_2 can significantly increase the cell performance. On the other hand, an important reduction of the solar cell efficiency is observed when sensitized electrodes are measured in closed cell configuration instead of three-electrode configuration, indicating that the counter electrode constitutes a limiting factor for the cell performance. Using impedance measurements we have found that the charge transfer resistance between the Pt and the polysulfide electrolyte is large, introducing a series resistance that deleteriously affects the cell behaviour.

Acknowledgments

The authors acknowledge Jan Kroon at ECN for providing the TiO_2 paste and Dirk Vanderzande at IMEC for discussions on cysteine properties. The work was supported by the Ministerio de Educación y Ciencia of Spain under projects HOPE CSD2007-00007 (Consolider-Ingenio 2010) and MAT2007-62982.

References

[1] O' Regan B and Grätzel M 1991 *Nature* **353** 737
[2] Grätzel M 2003 *J. Photochem. Photobiol.* **4** 145
[3] Bisquert J, Cahen D, Hodes G, Rühle S and Zaban A 2004 *J. Phys. Chem.* B **108** 8106
[4] Yu W, Qu L H, Guo W Z and Peng X G 2003 *Chem. Mater.* **15** 2854
[5] Wang P, Zakeeruddin S M, Moser J E, Humphry-Baker R, Comte P, Aranyos V, Hagfeldt A, Nazeeruddin M K and Grätzel M 2004 *Adv. Mater.* **16** 1806
[6] Klimov V I 2006 *J. Phys. Chem.* B **110** 16827
[7] Ellingson R J, Beard M C, Johnson J C, Yu P, Micic O I, Nozik A J, Shabaev A and Efros A L 2005 *Nano Lett.* **5** 865
[8] Schaller R D and Klimov V I 2004 *Phys. Rev. Lett.* **92** 186601
[9] Schaller R D, Sykora M, Pietryga J M and Klimov V I 2006 *Nano Lett.* **6** 424
[10] Franceschetti A, An J M and Zunger A 2006 *Nano Lett.* **6** 2191
[11] Nozik A J 2002 *Physica* E **14** 115
[12] Zaban A, Micic O I, Gregg B A and Nozik A J 1998 *Langmuir* **14** 3153
[13] Vogel R, Hoyer P and Weller H 1994 *J. Phys. Chem.* B **98** 3183
[14] Plass R, Pelet S, Krueger J and Grätzel M 2002 *J. Phys. Chem.* B **106** 7578
[15] Peter L M, Wijayantha K G U, Riley D J and Waggett J P 2003 *J. Phys. Chem.* B **107** 8378
[16] Yu P, Zhu K, Norman A G, Ferrere S, Frank A J and Nozik A J 2006 *J. Phys. Chem.* B **110** 25451
[17] Peter L M, Riley D J, Tull E J and Wijayantha K G U 2002 *Chem. Commun.* 1030
[18] Niitsoo O, Sarkar S K, Pejoux C, Rühle S, Cahen D and Hodes G 2006 *J. Photochem. Photobiol.* A **181** 306
[19] Robel I, Subramanian V, Kuno M and Kamat P V 2006 *J. Am. Chem. Soc.* **128** 2385

[20] López-Luque T, Wolcott A, Xu L P, Chen S, Wen Z, Li J, De la Rosa E and Zhang J Z 2008 *J. Phys. Chem.* C **112** 1282
[21] Leschkies S K, Divakar R, Basu J, Enache-Pommer E, Boercker J E, Carter C B, Kortshagen U R, Norris D J and Aydil E S 2007 *Nano Lett.* **7** 1793
[22] Kongkanand A, Tvrdy K, Takechi K, Kuno M and Kamat P V 2008 *J. Am. Chem. Soc.* **130** 4007
[23] Diguna L J, Shen Q, Kobayashi J and Toyoda T 2007 *Appl. Phys. Lett.* **91** 023116
[24] Liu C J, Olsen J, Sounders D R and Wang J H 1981 *J. Electrochem. Soc.* **128** 1224
[25] Ueno Y, Minoura H, Nishikawa T and Masayasu T 1983 *J. Electrochem. Soc.* **130** 43
[26] Daizadeh I, Medvedev D M and Stuchebrukhov A A 2002 *Mol. Biol. Evol.* **19** 406
[27] Lippard S J and Berg J M 1995 *Bioanorganische Chemie* (Heidelberg: Spektrum Akademischer Verlag)
[28] Tian Y, Shioda M, Kasahara S, Okajima T, Mao L, Hisabori T and Ohsaka T 2002 *Biochim. Biophys. Acta* **1569** 151
[29] Wang S and Du D 2002 *Sensors* **2** 41
[30] Rajh T, Ostafin A E, Micic O I, Tiede D M and Thurnauer M C 1996 *J. Phys. Chem.* **100** 4538
[31] Rajh T and Thurnauer M 2001 Semiconductor assisted metal deposition for nanolithography applications (Chicago, U.O., Ed., United States of America)
[32] Moehl T, Halim M A E and Tributsch H 2006 *J. Appl. Electrochem.* **36** 1341
[33] Moehl T 2005 Investigation of layered semiconductors by photoelectrochemical microwave reflection *PhD Thesis* Freie Universität, Chemistry
[34] Wang Q, Pan D, Jiang S, Ji X, An L and Jiang B 2006 *J. Cryst. Growth* **286** 83
[35] Zhao P, Zhang H, Zhou H and Yi B 2005 *Electrochim. Acta* **51** 1091
[36] Bakkers E P A M, Roest A L, Marsman A W, Jenneskens L W, de Jong-van Steensel L I, Kelly J J and Vanmaekelbergh D 2000 *J. Phys. Chem.* B **104** 7266
[37] Mora-Seró I, Bisquert J, Dittrich T, Belaidi A, Susha A S and Rogach A L 2007 *J. Phys. Chem.* C **111** 14889
[38] Fabregat-Santiago F, Bisquert J, Garcia-Belmonte G, Boschloo G and Hagfeldt A 2005 *Sol. Energy Mater. Sol. Cells* **87** 117
[39] Licht S, Khaselev O, Ramakrishnan P A, Soga T and Umeno M 1998 *J. Phys. Chem.* B **102** 2536
[40] Hodes G, Manassen J and Cahen D 1980 *J. Electrochem. Soc.* **127** 544